Supporting Information

Zhang et al. 10.1073/pnas.1009700107

SI Methods

Gene-Modified Mice. *Nox4*-null mice were generated by targeted deletion of the translation initiation site and exons 1 and 2 of the gene (Genoway). A 5′ murine Nox4 genomic DNA fragment was isolated from a 129sv DNA BAC library and used to generate a targeting construct containing exons 1 and 2 flanked by loxP sites, a negative-selection diptheria toxin A cassette and a positive selection neomycin cassette flanked by Flippase Recognition Target sites. The targeting construct was electroporated into 129sv embryonic stem cells, recombinant clones identified by PCR and Southern blot analysis, and injected into C57BL/6 blastocysts. Heterozygous mice obtained from germline chimeras were bred with C57BL/6 Cre-deletor mice and Flp-deletor mice to generate heterozygous knockout (KO) mice. *Nox4*-null animals were obtained by intercrossing progeny and were backcrossed >10 generations with C57BL/6 mice.

To generate cardiomyocyte-targeted *Nox4*-transgenic mice, the mouse Nox4 cDNA was cloned downstream of the mouse α-myosin heavy chain promoter (courtesy of J. Robbins, Children's Hospital, Cincinnati, OH). The construct was linearized and microinjected into fertilized CBA/C57BL/6 pronuclei. Positive founders were identified by PCR and were backcrossed for >10 generations onto a C57BL/6 background.

Aortic Constriction. All procedures were performed in accordance with the Guidance on the Operation of the Animals (Scientific Procedures) Act, 1986 (United Kingdom). We studied male *Nox4*-null mice or *Nox4*-transgenic mice and respective matched wild-type littermates, all on a C57BL/6 background. Aortic constriction was induced in ≈20-g mice by suprarenal banding under 2% isoflurane anesthesia, as previously described (1). Sham constriction involved identical surgery apart from band placement. Animals were studied up to 9 wk postsurgery. Aortic constriction resulted in similar rises in invasively measured systolic pressure among groups. There were no differences in mortality between mouse strains.

Echocardiography and Cardiac Hemodynamics. Mice were anesthetized with 1.5% isoflurane and imaged using a Sonos 5500 Imaging System with a 15-MHz linear transducer (Philips) or a Visualsonics Vevo 2100 ultrasound system with a 40-MHz transducer. For in vivo closed-chest LV pressure–volume analyses, animals were anesthetized with 2% isoflurane, and a 1.4F microconductance pressure catheter (ARIA SPR-853; Millar Instruments) was inserted via the right carotid artery into the left ventricle (LV) (2). Inferior vena cava occlusions were performed to generate end-systolic pressure–volume relations. Data were collected on Chart via Powerlab (Adinstruments) and analyzed using PVAN software (Millar Instruments). Heart rates were above 400 bpm in all experiments.

Real-Time RT-PCR. An Applied Biosystems PRISM 7700 machine was used with SYBR Green and the comparative cycle threshold method, with β-actin as internal controls. Oligonucleotide primers (forward, reverse) were the following: *Nox4* (mouse) TGAACTACAGTGAAGATTTCCTTGAAC, GACACCCGTCAGACCAGGAAT; *Nox4* (rat) GCCTAGGATTGTGTTTGAGCAGA, GCGAAGGTAAGCCAGGACTGT; *Hif1α* (mouse) CACCGATTCGCCATGGA, TTCGACGTTCAGAACTCATCTTTT; *Hif1α* (rat) GCTGCCTCTTCGACAAGCTT, CAGCCGCTGGAGCTAGCA; and *β-actin* CGTGAAAAGATGACCCAGATCA, TGGTACGACCAGAGGCATACAG.

Histology. Hearts that were in situ fixed in diastole were paraffin-embedded. To assess whole-heart morphology, longitudinal sections were prepared and stained with hematoxylin and eosin. For all other histology, 6-μm transverse cross-sections were used. FITC-conjugated wheat germ agglutinin (FITC-WGA, Vector RL-1022) was used to outline cardiomyocytes. Interstitial fibrosis was assessed by blinded quantitative image analysis (Openlab, Improvision) of Picrosirius red-stained sections (3). Capillaries were immunostained with isolectin B4 (Vector B-1205) and capillary density quantified as the number of capillaries per square millimeter (4). Apoptosis was assessed by TUNEL staining (Millipore S7110 kit). VEGF in the LV was detected with an anti-VEGF primary antibody, which was visualized with Alexa 568-conjugated anti-rabbit IgG (Molecular Probes).

Western Blotting and Protein Kinase Profiling. LV homogenates or cell lysates were separated by SDS/PAGE and transferred onto nitrocellulose membranes. Nuclear proteins were extracted as described (5). For the detection of hydroxylated Hif1α, Mg132 (5 μmol/L) was added immediately before cell lysis and also included in the lysis buffer. Antibodies used were the following: Nox4 (6); Nox2 and endothelial nitric oxide synthase (eNOS) (BD Transduction); $p22^{phox}$ (Santa Cruz Biotechnology); HIF-1α (Thermo Scientific); HIF-1α hydroxylated-Pro^{402} and -Pro^{564}, nitrotyrosine, and VEGF (Abcam); and pAkt (S473), pan-Akt, and histone-H3 (Cell Signaling). Actin (Sigma) was used as a loading control. Blots were quantified by densitometry. The protein kinase activity profiling screen was performed commercially (Kinetworks, Kinexus Bioinformatics).

Cultured Cardiomyocyte Studies. Primary cultures of neonatal rat cardiomyocytes (NRC) were prepared as described previously (7). Rat H9c2 cardiomyoblasts (ATCC) were cultured in DMEM high glucose supplemented with FBS (10%), streptomycin (100 μmol/L), and penicillin (100 U/mL). Adenoviral vectors expressing mouse Nox4 or β-galactosidase were generated using the AdEasy Adenoviral Vector System (Qbiogene), amplified in HEK293 cells, and isolated using the Adenopure virus purification kit (Puresyn). Cells were cultured for 24 h, infected with virus at an multiplicity of infection of 40 for 24 h, washed with PBS, and starved overnight before exposure to hypoxia. siRNA against Nox4 (sequence 5′-GCCUGAUCCUUUUACCCAUtt-3′) and a universal negative control were from Ambion. Serum and antibiotic-free siRNA–reduced serum minimum essential medium (OPTI-MEM, Invitrogen) complexes were incubated with cells for 24 h after which OPTI–MEM-free medium was replaced. Cells were used for experiments after an additional 24 h. To induce hypoxia, cells were placed in a hypoxia chamber (Stem Cell Technologies) flushed with a 95% N_2/4% CO_2/1% O_2 gas mixture for 24 h. Chemical hypoxia was induced by exposure to $CoCl_2$ (200 μmol/L). For VEGF detection in culture supernatants, equal volumes (10 mL) derived from NRC exposed to hypoxia were centrifuged (2,000 × *g* for 3 min) to pull down debris, and the supernatants were dried under vacuum (Speed Vac Plus model SC-110A, Thermo Savant). Pellets were resuspended in 0.1 mL water, protein content was estimated, and samples were submitted to the usual electrophoresis procedure.

Detection of ROS. H_2O_2 levels were detected with a homovanillic acid (HVA) assay by using the catalase-inhibitable signal (6). The assay was performed on NRC in six-well plates or using tissue minced into small pieces in 1 ml Hanks' balanced salt solution

with or without 750 U/mL catalase at 37 °C. HVA fluorescence was detected on a plate fluorimeter (Tecan GENios). H_2O_2 levels were estimated using a standard curve and normalized by protein content. Electron paramagnetic resonance spectroscopy (EPR) was used to measure O_2^- generation by heart particulate fractions (8). Briefly, the particulate fraction (80 μg) was incubated with the 5,5-dimethylpyrroline-*N*-oxide (DMPO; 50 mmol/L) spin trap in PBS containing diethylene triamine penta-acetic acid (100 μmol/L), pH 7.4, for 5 min at 37 °C. NADPH (0.6 mmol/L) was added and incubated for an additional 5 min, and spectra were recorded in a Magnettech Miniscope MS2000 spectrometer. Instrument conditions were the following: microwave power—50 mW and modulation amplitude—1 Gauss (G), with a gain of 9×10^2. The four-line spectrum (solid circle in Fig. S2*B*) is consistent with a DMPO-hydroxy (DMPO-OH) radical adduct (a_N = 14.9 G and a_H= 14.9 G) as generated using the positive control of xanthine (0.1 mmol/L)/xanthine oxidase (0.05 U/mL) under similar conditions. The DMPO-OH adduct was quantified by assessing the height of the second peak as a linear function, using 4-hydroxy-2,2,6,6-tetramethyl-1-piperidinyloxy (Tempol) as a standard.

Immunostaining. Adult cardiomyocytes were isolated from adult *Nox4*-transgenic and wild-type mice using collagenase digection. Cells were plated onto laminin-pretreated slides, fixed, and permeabilized. After incubation with primary antibody or nonspecific IgG, bound antibodies were visualized with Alexa 488 conjugated anti-rabbit or Alexa 568 conjugated anti-mouse IgG (Molecular Probes). Imaging was done on a Leica laser scanning confocal microscope (TCS-SP5).

Endothelial Tube Formation Assay. The cell culture supernatants (conditioned media) of NRC were used for in vitro endothelial tube formation assays. Human umbilical vein endothelial cells (HUVECs) were seeded on Matrigel-coated eight-well chamber slides and incubated with 0.4 mL conditioned medium for 4 h at 37 °C, with or without VEGF blocking antibody (2 μg/mL; R&D System, AF564) or nonspecific IgG. Tube formation was examined by phase-contrast microscopy, and Axiovision software (Carl Zeiss) was used to quantify tube formation (9). The length of tubes in three to four randomly selected fields in each well was measured and compared with untreated HUVECs.

Statistics. Data are presented as mean ± SEM. Comparisons of groups were undertaken by Student's *t* test or one-way ANOVA, as appropriate. A post hoc Tukey's test was performed to isolate differences. $P < 0.05$ was considered significant.

1. Byrne JA, et al. (2003) Contrasting roles of NADPH oxidase isoforms in pressure-overload versus angiotensin II-induced cardiac hypertrophy. *Circ Res* 93:802–805.
2. Georgakopoulos D, et al. (1998) In vivo murine left ventricular pressure-volume relations by miniaturized conductance micromanometry. *Am J Physiol* 274:H1416–H1422.
3. Looi YH, et al. (2008) Involvement of Nox2 NADPH oxidase in adverse cardiac remodeling after myocardial infarction. *Hypertension* 51:319–325.
4. Hilfiker-Kleiner D, et al. (2007) A cathepsin D-cleaved 16 kDa form of prolactin mediates postpartum cardiomyopathy. *Cell* 128:589–600.
5. Novoa I, Zeng H, Harding HP, Ron D (2001) Feedback inhibition of the unfolded protein response by GADD34-mediated dephosphorylation of eIF2alpha. *J Cell Biol* 153:1011–1022.
6. Anilkumar N, Weber R, Zhang M, Brewer A, Shah AM (2008) Nox4 and nox2 NADPH oxidases mediate distinct cellular redox signaling responses to agonist stimulation. *Arterioscler Thromb Vasc Biol* 28:1347–1354.
7. Zhang M, et al. (2006) Glycated proteins stimulate reactive oxygen species production in cardiac myocytes: Involvement of Nox2 (gp91phox)-containing NADPH oxidase. *Circulation* 113:1235–1243.
8. Janiszewski M, et al. (2005) Regulation of NAD(P)H oxidase by associated protein disulfide isomerase in vascular smooth muscle cells. *J Biol Chem* 280:40813–40819.
9. Prokopi M, et al. (2009) Proteomic analysis reveals presence of platelet microparticles in endothelial progenitor cell cultures. *Blood* 114:723–732.

Fig. S1. Increase in cardiac Nox4 during pressure overload and generation of *Nox4*-null mice. (*A*) Nox4 protein expression in heart after aortic banding (Band) or control surgery (Sham) shown by Western blots. LV sections show immunostaining for Nox4 (1, Sham; 2, Band; 3, Band + blocking antigenic peptide). Mean data are in bar graph. Scale bar: 20 μm. $^{**}P < 0.01$; $n = 4$/group. (*B*) Targeting strategy for generation of *Nox4*-null mice. Southern blots, performed after excision at *AvrII* sites, show 9.3- and 3.2-kb bands in heterozygous knockout (Het) mice but only the 9.3-kb band in WT. The 5′ *AvrII* site in the knockout allele is produced by the targeted deletion.

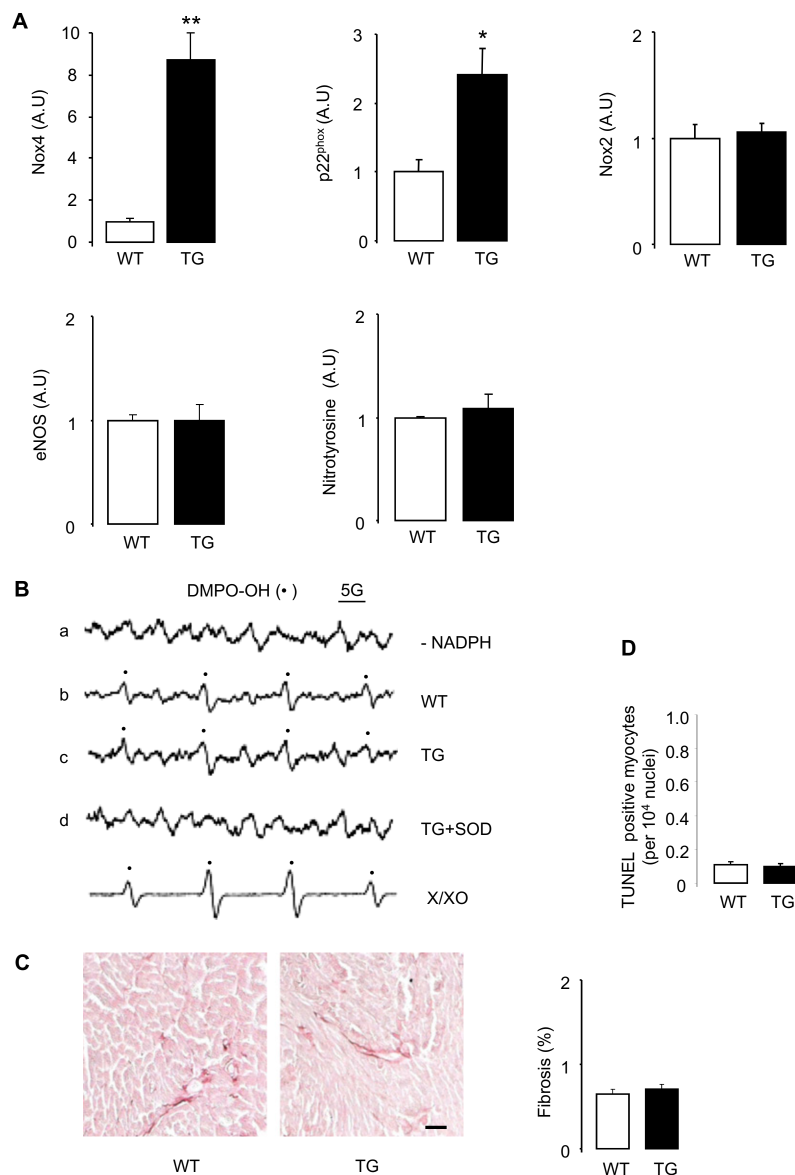

Fig. S2. Basal phenotype of *Nox4*-transgenic mice (TG). (*A*) Quantification of protein levels of Nox4, p22^{phox}, Nox2, eNOS, and nitrotyrosine in hearts of *Nox4*-TG and wild-type littermates (WT). $**P < 0.01$; $*P < 0.05$; $n = 3$/group. (*B*) EPR spectra for detection of O_2^- in heart. The four-line spectrum (•) is consistent with the DMPO-OH radical adduct (a_N = 14.9 G and a_H= 14.9 G), as confirmed by a xanthine (0.1 mmol/L)/xanthine oxidase (0.05 U/mL) positive control under similar conditions. Inhibition of signal by superoxide dismutase (SOD) was used to confirm specificity. Measurements were made in the presence of NADPH (0.6 mmol/L) except where indicated. Mean yields (arbitrary units) from three independent experiments were the following: a and d, undetectable; b, WT = 1.50 ± 0.21; c,TgNox4 = 1.6 ± 0.31; *P* = NS. (*C*) Lack of increase in interstitial fibrosis in 12-mo-old *Nox4*-transgenic mice. Representative LV sections stained with Picrosirius red (scale bar: 50 μm) and mean data from seven to nine mice/group. (*D*) Quantification of TUNEL staining in LV sections of 12-mo-old *Nox4*-transgenic mice and wild-type littermate controls (seven to nine mice/group).

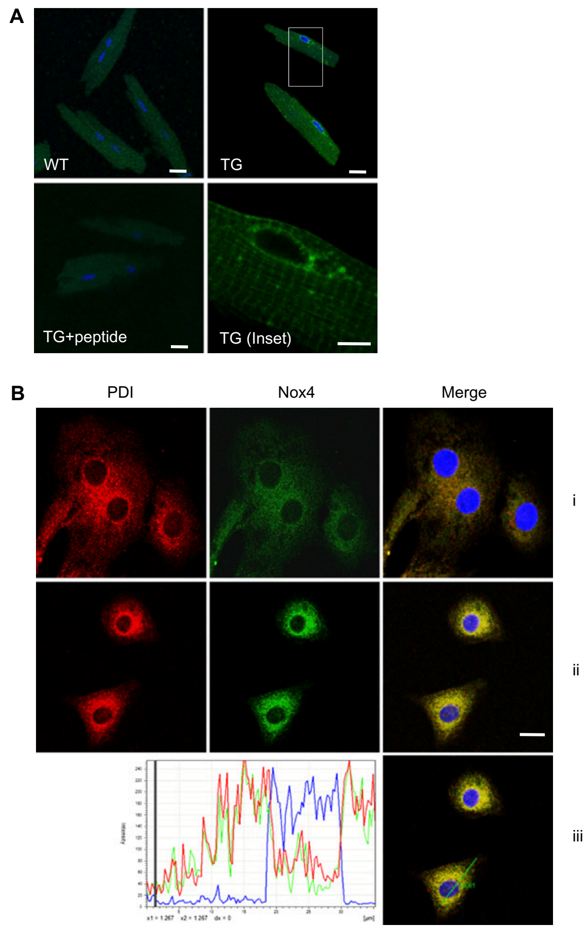

Fig. S3. Immunostaining for Nox4 in cardiomyocytes. (*A*) Nox4 immunostaining (green) in myocytes from *Nox4*-transgenic and wild-type hearts. (*Lower right*) A higher magnification of the boxed area in *Upper right*. Scale bars: 20 μm and 5 μm, respectively. Specificity of immunostaining was confirmed with a blocking antigenic peptide (*Lower left*). Cardiomyocyte nuclei were stained with DAPI (blue). (*B*) Nox4 staining in cultured cardiomyocytes. (i) Endogenous Nox4 in neonatal rat cardiomyocytes. (ii) Cells infected with a Nox4-expressing adenovirus. Cells were stained for Nox4 and for protein disulfide isomeriase (PDI) as an endoplasmic reticulum marker. Yellow color in the merged images indicates colocalization. Scale bar: 20 μm. (iii) The panel at the left shows pixel-by-pixel fluorescence intensities of the two fluorophores in the cell shown at the right, along an arbitrary line, assessed using the Leica TCS-SP5 software. A significant overlapping pattern was found between Nox4 and PDI.

Fig. S4. *Nox4*-transgenic mice are protected against pressure overload-induced cardiac dysfunction and remodeling. (*A*) Echocardiographic analyses. Representative M-mode traces are shown at the left. Mean data from >15 animals per group are shown at the right. IVSD, interventricular septal thickness in diastole; LVEDD, LV end-diastolic diameter; LVESD, LV end-systolic diameter; FS, % fractional shortening. $^{**}P < 0.01$ and $^{*}P < 0.05$ for band vs. respective sham; $^{\#\#}P < 0.01$ for TG band vs. WT band. (*B*) Representative longitudinal sections of hearts of animals subjected to pressure overload or sham surgery. Scale bar: 2 mm. (*C*) Reduced cardiomyocyte hypertrophy after pressure overload in *Nox4*-transgenic mice: representative WGA-stained LV sections. Scale bar: 20 μm. (*D*) Reduced fibrosis in LV of *Nox4*-transgenic mice: representative Picrosirius red-stained sections. Scale bar: 20 μm.

Fig. S5. Protection against load-induced stress in a second line of *Nox4*-transgenic mice. (*A*) Western blots showing Nox4 expression in heart of two independent transgenic mouse lines. Myocardial Nox4 protein levels were 7.7- ± 1.1-fold higher in transgenic mice of line 2 vs. wild type ($n = 3$). Data for line 1 are shown in the main text and in Figs. S2–S4. (*B*) Effect of chronic pressure overload (Band) on WT and *Nox4*-transgenic (TG) mice from line 2. Sham denotes control groups. HW/BW, heart weight/body weight ratio; LV/BW, left ventricular/body weight; IVSD, interventricular septal thickness in diastole; LVESD, LV endsystolic diameter; LVEDD, LV end-diastolic diameter; FS, fractional shortening. $^{**}P < 0.01$ for band vs. respective sham; $^{\#}P < 0.05$; $^{\#\#}P < 0.01$ for TG band vs. WT band; $n \geq 7$/group. (*C*) Changes in phosphorylated Akt (P-Akt; S473) and total Akt (T-Akt) in LV of *Nox4*-transgenic (*Left*) and *Nox4*-null mice (*Right*) compared with respective wild-type littermates. (*Upper Left* and *Upper Right*) Representative immunoblots. (*Lower Left* and *Lower Right*) mean data. $^{\#}P < 0.05$ for TG Band vs. WT Band; $n = 4$/group.

Fig. S6. Regulation of VEGF and Hif1a by Nox4. (*A*) Immunostaining for VEGF in LV sections of WT, TG and KO mice. (Scale bar 50 μm.) (*B*) Mean data from experiments with Nox4 overexpression in cardiomyocytes illustrated in Fig. 6*A*. ** *P*< 0.01 for Nox4 hypoxia vs. normoxia; #*P* < 0.05 for Nox4 vs. β-gal; *n* = 3/group. (*C*) H_2O_2 generation by Nox4 compared to β-gal-overexpressing cardiomyocytes. ***P* < 0.01; *n* = 3/group. (*D*, *E*) Hif1a mRNA levels in LV of *Nox4*-transgenic mice (*D*) or *Nox4*-null mice (*E*) compared to respective WT. **P* < 0.05 for band vs. respective sham; #*P* < 0.05 for TG vs. respective WT; *n* = 4/group. (*F*) Effect of Nox4 or β-gal on Hif1a mRNA levels in cardiomyocytes during normoxia or hypoxia. *n* = 6/group. (*G*) Representative phase contrast micrographs showing the effect of cardiomyocyte-conditioned medium of 1, control (β-gal-expressing) myocytes; 2, Nox4-overexpressing myocytes; 3, Nox4-overexpressing myocytes plus a VEGF-blocking antibody; 4, Nox4-overexpressing myocytes plus non-specific IgG; on endothelial cell tube formation.

Table S1. Baseline phenotype of *Nox4*-null mice aged 2 mo

	WT (*n* = 23)	KO (*n* = 21)
Body weight (g)	18.2 ± 0.3	18.9 ± 0.4
Heart weight (g)	0.112 ± 0.003	0.116 ± 0.004
Kidney weight (g)	0.237 ± 0.07	0.240 ± 0.01
Lung weight (g)	0.166 ± 0.011	0.154 ± 0.005
Liver weight (g)	0.935 ± 0.030	0.978 ± 0.038
Spleen weight (g)	0.079 ± 0.003	0.074 ± 0.002
Blood pressure (mmHg)	97 ± 1	98 ± 1

Table S2. Basal characterization of *Nox4*-transgenic mice compared with WT littermates at ages 3 and 12 mo

	3 mo		12 mo	
	WT (*n* = 13)	TG (*n* = 13)	WT (*n* = 9)	TG (*n* = 7)
BW (g)	25.8 ± 0.4	25.0 ± 0.3	40.4 ± 2.4	40.4 ± 2.6
HW/BW (mg/g)	4.53 ± 0.07	4.75 ± 0.05	3.62 ± 0.09	4.07 ± 0.13*
LV/BW (mg/g)	3.47 ± 0.05	3.57 ± 0.05	2.84 ± 0.06	3.18 ± 0.11*
HR (beats/min)	426 ± 13	409 ± 11	460 ± 17	489 ± 19
IVSD (mm)	0.76 ± 0.01	0.80 ± 0.01	0.90 ± 0.05	1.09 ± 0.07*
LVESD (mm)	2.55 ± 0.03	2.34 ± 0.07	2.91 ± 0.10	2.79 ± 0.10
LVEDD (mm)	4.13 ± 0.03	4.10 ± 0.07	4.19 ± 0.09	3.99 ± 0.08
FS (%)	38.3 ± 0.5	42.9 ± 1.1*	30.8 ± 1.4	30.2 ± 1.4

BW, body weight; HW, heart weight; HR, heart rate; IVSD, interventricular septal thickness in diastole; LVEDD, LV end-diastolic diameter; LVESD, LV end-systolic diameter; FS, fractional shortening. Data are means ± SEM.
*$P < 0.05$ compared with respective WT littermates.